Arab J Math (2013) 2:263–277
DOI 10.1007/s40065-013-0072-3

Ahmed A. Khidir

Viscous dissipation, Ohmic heating and radiation effects on MHD flow past a rotating disk embedded in a porous medium with variable properties

Received: 30 October 2012 / Accepted: 5 April 2013 / Published online: 24 April 2013

Abstract The present work investigates the effects of viscous dissipation and Ohmic heating on steady MHD convective flow due to a porous rotating disk taking into account the variable fluid properties (density (ρ) viscosity (μ) and thermal conductivity (κ)) in the presence of Hall current and thermal radiation. These properties are taken to be dependent on temperature. The partial differential equations governing the problem under consideration are reduced to a system of BVP ordinary differential equations by using similarity transformations which are solved numerically using the successive linearization method. Comparisons with previously published works are performed to test the validity of the obtained results. The effects of different parameters on the velocity as well as temperature are depicted graphically and are analyzed in detail and the numerical values of the skin friction and the rate of heat transfer are entered in tables.

Mathematics Subject Classification 76S99

الملخص

في هذا العمل نقوم بالتحقيق في آثار تخميد لزج وحرارة أومنية (Ohmic) على تدفق MHD ثابت وناتج عن دوران قرص مسامي آخذين بعين الاعتبار خصائص السائل المتغيرة (الكثافة (ρ) واللزوجة (μ) والتوصيل الحراري (κ)) أثناء وجود تيار Hall وإشعاع حراري. هذه الخصائص أخذت مستقلة عن الحرارة. لقد تمَّ اختزال المعادلات التفاضلية الجزئية المنمذجة للمسألة تحت النظر إلى مسألة قيم حدية لنظام معادلات تفاضلية عادية وذلك باستخدام تحويلات التشابه والتي تمَّ حلّها عدديا بطريقة الخطية المتعاقبة. كما أجريت بعض المقارنات مع أعمال منشورة سابقا لاختبار صحة النتائج التي تم الحصول عليها. لقد تمَّت متابعة آثار الوسائط (البرامترات) المختلفة على السرعة والحرارة بالمنحنيات وحللت تفصيليا كما تمَّ إدخال القيم العددية لاحتكاك الجلد ومعدل انتقال الحرارة في جداول.

1 Introduction

The study of rotating disk flows of electrically conducting fluids along with heat transfer is one of the classical problems of fluid mechanics and has many applications in many areas. The original problem of rotating-disk was raised by von-Karman [32]. He introduced the equations of Navier–Stokes of steady flow of a viscous incompressible fluid due to a rotating disk to a set of ordinary differential equations and solved them by means of the momentum integral method. Further Cochran [7] improved the result of von-Karman and obtained asymptotic solutions for the reduced system of ordinary differential equations and also gave more accurate results by patching two series expansions. The solution of Cochran has been improved by Benton [6] who extended the hydrodynamic problem to the flow starting impulsively from rest. Turkyilmazoglu [30,31]

A. A. Khidir (✉)
Faculty of Technology of Mathematical Sciences and Statistics, Alneelain University,
Algamhoria Street, P.O. Box 12702, Khartoum, Sudan
E-mail: ahmed.khidir@yahoo.com

extended the classical von-Karman problem of flow over a rotating disk to account for compressibility effects with insulated and isothermal wall conditions. He used an exponentially decaying series method to find the solution of the steady laminar flow of an incompressible, viscous, electrically-conducting fluid over a rotating disk in the presence of a uniform transverse magnetic field. Millsaps and Pohlhausen [19] considered the problem of heat transfer from a rotating disk maintained at a constant temperature for a variety of Prandtl numbers in steady state. Attia [3] extended the problem studied by Millsaps and Pohlhausen [19] and Sparrow and Gregg [28] to the unsteady state in the presence of an applied uniform magnetic field and he obtained a numerical solution for the governing equations. Sibanda and Makinde [27] investigated the heat transfer characteristics of steady MHD flow in a viscous electrically conducting incompressible fluid with Hall current past a rotating disk with ohmic heating and viscous dissipation. They found that the magnetic field retards the fluid motion due to the opposing Lorentz force generated by the magnetic field.

In the above-mentioned studies, the fluid properties are taken to be constant (namely density, viscosity and thermal conductivity). The effects of variable properties on laminar flow over a rotating disk have been considered, among others. The study of Attia [4] considered the effect of a porous medium and temperature-dependent viscosity on the unsteady flow and heat transfer for a viscous laminar incompressible fluid due to an impulsively started rotating disc. The effects of variable properties and hall current on steady MHD laminar convective fluid flow due to a porous rotating disk were investigated by Maleque and Sattar [17]. The effects of variable properties on a steady laminar forced convection system along a porous rotating disk with uniform temperature were investigated by Maleque and Sattar [18]. They reported that for fixed values of the suction parameter and Prandtl number, the momentum boundary layer increased considerably while the thermal boundary layer is found to vary little with variable properties. Then, their work was extended by Osalusi and Sibanda [23] to include the effects of an applied magnetic field. Frusteri and Osalusi [10] carried out the study of magnetic effects on electrically conducting fluid in slip regime with variable properties. The flow field on a single porous rotating disk with heat transfer was studied. They showed that the radial and tangential velocity profiles are reduced by both slip coefficient and magnetic field. Osalusi et al. [24] discussed the effects of Ohmic heating and viscous dissipation on unsteady hydro-magnetic and slip flow of a viscous fluid over a porous rotating disk in the presence of Hall and ion-slip currents taking into account the variable properties of the fluid.

The purpose of the present study is to investigate the combined effects of viscous dissipation, Ohmic heating and radiation on a MHD porous rotating disk by considering the variable properties of density, viscosity and thermal conductivity in the presence of Hall current, permeability and radiation. A uniform suction or injection is applied through the surface of the disk.

The governing equations for this investigation are modified to include radiation, Ohmic heating and viscous dissipation effects with the generalized Ohm's and Maxwell's laws. They were solved using a novel successive linearization method (SLM). This new technique has been successfully applied to different fluid flow problems. Makukula et al. [13] solved the classical von Karman equations governing boundary layer flow induced by a rotating disk using the spectral homotopy analysis method and SLM. Makukula et al. [14] applied the SLM on the problem of the heat transfer in a visco-elastic fluid between parallel plates and compared their solution with the improved spectral homotopy analysis method (ISHAM). They showed that the rate of convergence of the SLM and ISHAM approximations convergence rapidly to the exact result. Many investigations, such as those by Makukula et al. [15,16], Awad et al. [5], Motsa and Sibanda [20], Motsa et al. [21,22] and Shateyi and Motsa [26], used SLM to solve different equations of boundary value problems. They compared their results with different methods and showed that the SLM gives better accuracy at lower orders, is more efficient, is generally applicable, gives rapid convergence and is, thus, superior to some existing semi-analytical methods, such as the Adomian decomposition method, the Laplace transform decomposition technique, the variational iteration method and the homotopy perturbation method. The SLM method can be used in the place of traditional numerical methods such as finite differences, Runge–Kutta shooting methods, and finite elements in solving non-linear boundary value problems.

2 Problem statement and mathematical formulation

In this investigation, we consider the problem of steady hydromagnetic convective and slip flow due to a rotating disk in the presence of viscous dissipation, radiation and Ohmic heating. Using non-rotating cylindrical polar coordinates (r, ϕ, z) the disk rotates with constant angular velocity Ω and is placed at $z = 0$, and the fluid occupies the region $z > 0$ where z is the vertical axis in the cylindrical coordinates system with r and ϕ as

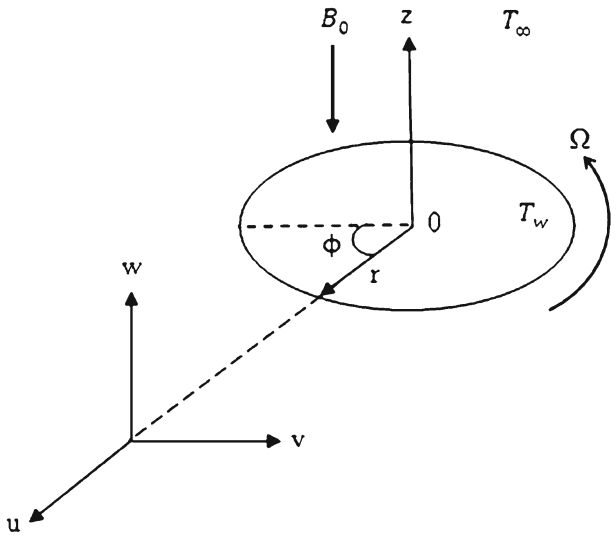

Fig. 1 Coordinate system for the rotating disk flow

the radial and tangential axes, respectively, as indicated in Fig. 1. The fluid velocity components are (u, v, w) in the directions of (r, ϕ, z), respectively, the pressure is P, the density of the fluid is ρ and T is the fluid temperature. The surface of the rotating disk is maintained at a uniform temperature T_w. Far away from the wall, the free stream is kept at a constant temperature T_∞ and at constant pressure P_∞. The external uniform magnetic field is applied perpendicular to the surface of the disk and has a constant magnetic flux density B_0 which is assumed unchanging with a small magnetic Reynolds number ($Re_m \ll 1$). We assume that the fluid properties, viscosity (μ) and thermal conductivity (κ) coefficients and density (ρ) are functions of temperature alone and obey the following laws (see Maleque and Sattar [17], Osalusi and Sibanda [25], Jayaraj [11])

$$\mu = \mu_\infty [T/T_\infty]^a, \qquad \kappa = \kappa_\infty [T/T_\infty]^b, \qquad \rho = \rho_\infty [T/T_\infty]^c \tag{1}$$

where a, b and c are arbitrary exponents, κ_∞ is a uniform thermal conductivity of heat, and μ_∞ is a uniform viscosity of the fluid. For the present analysis fluid considered is flue gas. For flue gases the values of the exponents a, b and c are taken as $a = 0.7$, $b = 0.83$ and $c = -1$. The case $c = -1$ is that of an ideal gas. The physical model and geometrical coordinates are shown in Fig. 1. The equations governing the motion of the MHD laminar flow of the homogeneous fluid take the following form

$$\frac{\partial}{\partial r}(\rho r u) + \frac{\partial}{\partial z}(\rho r w) = 0, \tag{2}$$

$$\rho\left(u\frac{\partial u}{\partial r} - \frac{v^2}{r} + w\frac{\partial u}{\partial z}\right) + \frac{\partial P}{\partial r} + \frac{\mu}{K}u = \frac{\partial}{\partial r}\left(\mu\frac{\partial u}{\partial r}\right) + \frac{\partial}{\partial r}\left(\mu\frac{u}{r}\right) + \frac{\partial}{\partial z}\left(\mu\frac{\partial u}{\partial z}\right) - \frac{\sigma B_0^2}{\alpha^2+\beta_e^2}(\alpha u - \beta_e v), \tag{3}$$

$$\rho\left(u\frac{\partial v}{\partial r} - \frac{uv}{r} + w\frac{\partial v}{\partial z}\right) + \frac{\mu}{K}v = \frac{\partial}{\partial r}\left(\mu\frac{\partial v}{\partial r}\right) + \frac{\partial}{\partial r}\left(\mu\frac{v}{r}\right) + \frac{\partial}{\partial z}\left(\mu\frac{\partial v}{\partial z}\right) - \frac{\sigma B_0^2}{\alpha^2+\beta_e^2}(\alpha v + \beta_e u), \tag{4}$$

$$\rho\left(u\frac{\partial w}{\partial r} + w\frac{\partial w}{\partial z}\right) + \frac{\partial P}{\partial r} + \frac{\mu}{K}w = \frac{\partial}{\partial r}\left(\mu\frac{\partial w}{\partial r}\right) + \frac{1}{r}\frac{\partial}{\partial r}(\mu w) + \frac{\partial}{\partial z}\left(\mu\frac{\partial w}{\partial z}\right), \tag{5}$$

$$\rho C_p\left(u\frac{\partial T}{\partial r} + w\frac{\partial T}{\partial z}\right) = \frac{\partial}{\partial r}\left(\kappa\frac{\partial T}{\partial r}\right) + \frac{\kappa}{r}\frac{\partial T}{\partial r} + \frac{\partial}{\partial z}\left(\kappa\frac{\partial T}{\partial z}\right) - \frac{\partial q_r}{\partial z} + \mu\left[\left(\frac{\partial u}{\partial r}\right)^2 + \left(\frac{\partial v}{\partial z}\right)^2\right] + \frac{\sigma B_0^2}{\alpha^2+\beta_e^2}(u^2+v^2), \tag{6}$$

where $\sigma\ \left(= \left(e^2 n_e t_e\right)/m_e\right)$ is the electrical conductivity, e is the electron charge, n_e is the electron number density, t_e is the electron collision time and m_e is the mass of the electron. C_p is the specific heat at constant pressure of the fluid, $\alpha = 1 + \beta_i\beta_e$, $\beta_e\ (= \omega_e t_e)$ is the Hall parameter which may be positive or

negative depending on the orientation of the magnetic field, ω_e $(= eB_0/m_e)$ is the electron frequency, and β_i $(= en_eB_0/((1 + n_e/n_a)K_{ai}))$ is the ion-slip parameter, n_a is the neutral particle number density, K_{ai} is the friction coefficient between ions and neutral particles and K is the Darcy permeability parameter. The last two terms on the right-hand side of the energy equation (6) denote the magnetic and viscous heating terms, respectively, q_r is the radiative heat flux. The appropriate boundary conditions for the flow induced by an infinite disk $(z = 0)$ which rotates with constant angular velocity Ω subjected to uniform suction/injection W_s through the disk can be introduced as follows

$$\left.\begin{array}{llll} u = 0, & v = \Omega r, & w = W_s & T = T_w, \quad \text{at} \quad z = 0, \\ u \to 0, & v \to 0, & T \to T_\infty, & P \to P_\infty \quad \text{as} \quad z \to \infty. \end{array}\right\} \tag{7}$$

By using the Rosseland approximation [1] for radiation for an optically thick layer we can write

$$q_r = -\frac{4\sigma^*}{3k^*}\frac{\partial T^4}{\partial z}, \tag{8}$$

where σ^* is the Stefan–Boltzmann constant and k^* is the mean absorption coefficient. We assumed that the temperature differences within the flow are such that the term T^4 may be expressed as a linear function of temperature. This is accomplished by expanding T^4 in a Taylor series about T_∞ and neglecting second and higher order terms, we get

$$T^4 \cong 4T_\infty^3 T - 3T_\infty^4 \tag{9}$$

then

$$\frac{\partial q_r}{\partial z} = -\frac{16\sigma^* T_\infty^3}{3k^*}\frac{\partial^2 T}{\partial z^2}, \tag{10}$$

3 Similarity transformation

The solutions of the governing equations are obtained by introducing a dimensionless normal distance from the disk, $\eta = z(\Omega/\mu_\infty)^{1/2}$ along with the von Karman transformations with the following representations for the radial, tangential and axial velocities, pressure and temperature distributions

$$\left.\begin{array}{lll} u = \Omega r F(\eta), & v = \Omega r G(\eta), & w = (\Omega\mu_\infty)^{\frac{1}{2}} H(\eta) \\ P - P_\infty = 2\mu_\infty \Omega p(\eta), & \text{and} & T - T_\infty = \Delta T\theta(\eta) \end{array}\right\} \tag{11}$$

where μ_∞ is a uniform kinematic viscosity of the fluid and $\Delta T = Tw - T_\infty$. Substituting these transformations into Eqs. (2)—(6) gives the nonlinear ordinary differential equations,

$$H' + 2F + c\epsilon H\theta'(1 + \epsilon\theta)^{-1} = 0, \tag{12}$$

$$F'' - Da^{-1}F - (1 + \epsilon\theta)^{-a}\frac{M}{\alpha^2 + \beta_e^2}[\alpha F - \beta_e G] - (1 + \epsilon\theta)^{c-a}\left[F^2 - G^2 + HF'\right]$$
$$+a\epsilon(1 + \epsilon\theta)^{-1}\theta' F' = 0, \tag{13}$$

$$G'' - Da^{-1}G - (1 + \epsilon\theta)^{c-a}\left[2FG + HG'\right] - (1 + \epsilon\theta)^{-a}\frac{M}{\alpha^2 + \beta_e^2}[\alpha G + \beta_e F] \tag{14}$$
$$+a\epsilon(1 + \epsilon\theta)^{-1}\theta' G' = 0, \tag{15}$$

$$\left(1 + \frac{4}{3R_d}(1 + \epsilon\theta)^{-b}\right)\theta'' - Pr(1 + \epsilon\theta)^{c-b}H\theta' + b\epsilon(1 + \epsilon\theta)^{-1}\theta'^2 + \frac{PrEcM}{\alpha^2 + \beta_e^2}(1 + \epsilon\theta)^{-b}\left[F^2 + G^2\right]$$
$$+EcPr(1 + \epsilon\theta)^{a-b}\left[F'^2 + G'^2\right] = 0 \tag{16}$$

The physical parameters appearing in Eqs. (12)–(16) are defined as follows

$$\left.\begin{array}{llll} M = \frac{\sigma B_0^2}{\rho_\infty \Omega}, & Pr = \frac{\mu_\infty C_p}{\kappa_\infty}, & Ec = \frac{r^2\Omega^2}{C_p\Delta T}, & R_d = \frac{\kappa_\infty k^*}{4\sigma^* T_\infty^3}, \quad Da = \frac{K\Omega}{\mu} \end{array}\right\} \tag{17}$$

Table 1 Comparison of current and previous studies of the $F'(0)$, $-G'(0)$ and $\theta'(0)$ obtained when $M = 0$, $Da = 0$, $R_d = 0$; $\epsilon = 0$, $Ec = 0$ and $Pr = 0.71$

h_w	Kelson and Desseaux [12]			Present results		
	$F'(0)$	$-G'(0)$	$-\theta'(0)$	$F'(0)$	$-G'(0)$	$-\theta'(0)$
3	0.309147	$0.602893e^{-1}$	$0.576744e^{-3}$	0.309148	$0.602893e^{-1}$	$0.580755e^{-3}$
2	0.398934	0.135952	$0.110135e^{-1}$	0.398934	0.135952	$0.110445e^{-1}$
0	0.489481	0.302173	$0.848848e^{-1}$	0.489481	0.302173	$0.849614e^{-1}$
−1	0.389569	1.175222	0.793048	0.389569	1.175224	0.793054
−2	0.242421	2.038527	1.437782	0.242425	2.038530	1.437785
−3	0.165582	3.012142	2.135585	0.165591	3.012144	2.135587

where M is the magnetic interaction parameter that represents the ratio of the magnetic force to the fluid inertial, Pr is the Prandtl number, Ec is the Eckert number that characterizes dissipation, R_d is the radiation parameter, Da is the local Darcy number and $\epsilon = \Delta T/T$ which is the relative temperature difference parameter, which is positive for heated surface, negative for a cooled surface and zero for uniform properties. The prime symbol indicates derivative with respect to η. The boundary conditions (7) transform to

$$\left.\begin{array}{llll} F(0) = 0, & G(0) = 1, & H(0) = h_w, & \theta(0) = 1, \quad \text{at} \quad \eta = 0, \\ F(\infty) = 0, & G(\infty) = 0, & H(\infty) = 0, & \theta(\infty) = 1, \quad \text{as} \quad \eta \to \infty. \end{array}\right\} \tag{18}$$

where $h_w = W_s/\sqrt{\nu_\infty \Omega}$ represents a uniform suction ($h_w > 0$) or injection ($h_w < 0$) at the disk (see [12]). The boundary conditions given by Eq. (18) imply that the radial (F), the tangential (G) components of velocity and temperature vanish sufficiently far away from the disk, whereas the axial velocity component (H) is anticipated to approach a yet unknown asymptotic limit for sufficiently large η-values. The skin friction coefficients to the surface ($\eta = 0$) are obtained by applying the following Newtonian formulas

$$\tau_t = \left[\mu\left(\frac{\partial v}{\partial z} + \frac{1}{r}\frac{\partial w}{\partial \phi}\right)\right]_{z=0} = \mu_\infty (1+\epsilon)^a Re^{\frac{1}{2}} \Omega G'(0),$$
$$\tau_r = \left[\mu\left(\frac{\partial u}{\partial z} + \frac{\partial w}{\partial r}\right)\right]_{z=0} = \mu_\infty (1+\epsilon)^a Re^{\frac{1}{2}} \Omega F'(0).$$

and we use Fourier's law

$$q = -\left(\kappa \frac{\partial T}{\partial z}\right) = -\kappa_\infty \Delta T (1+\epsilon)^b \left(\frac{\Omega}{\nu_\infty}\right)^{\frac{1}{2}} \theta'(0), \tag{19}$$

to find the rate of heat transfer from the disk surface to the fluid. Hence the tangential, radial skin-frictions and Nusselt number Nu are, respectively, given by

$$(1+\epsilon)^{-a} Re^{\frac{1}{2}} C_{f_t} = G'(0), \tag{20}$$
$$(1+\epsilon)^{-a} Re^{\frac{1}{2}} C_{f_r} = F'(0), \tag{21}$$
$$(1+\epsilon)^{-b} Re^{\frac{1}{2}} = -\theta'(0), \tag{22}$$

where $Re(= \Omega r^2/\nu_\infty)$ is the rotational Reynolds number.

4 Method of solution

In this work we applied the SLM to solve the system of ordinary differential equations (12)–(16). The SLM is based on the assumption that the unknown functions $H(\eta)$, $F(\eta)$, $G(\eta)$ and $\theta(\eta)$ can be expanded as

$$\left.\begin{array}{ll} H(\eta) = H_i(\eta) + \sum_{m=0}^{i-1} H_m(\eta), & F(\eta) = F_i(\eta) + \sum_{m=0}^{i-1} F_m(\eta), \\ G(\eta) = G_i(\eta) + \sum_{m=0}^{i-1} G_m(\eta), & \theta(\eta) = \theta_i(\eta) + \sum_{m=0}^{i-1} \theta_m(\eta), \end{array}\right\} \tag{23}$$

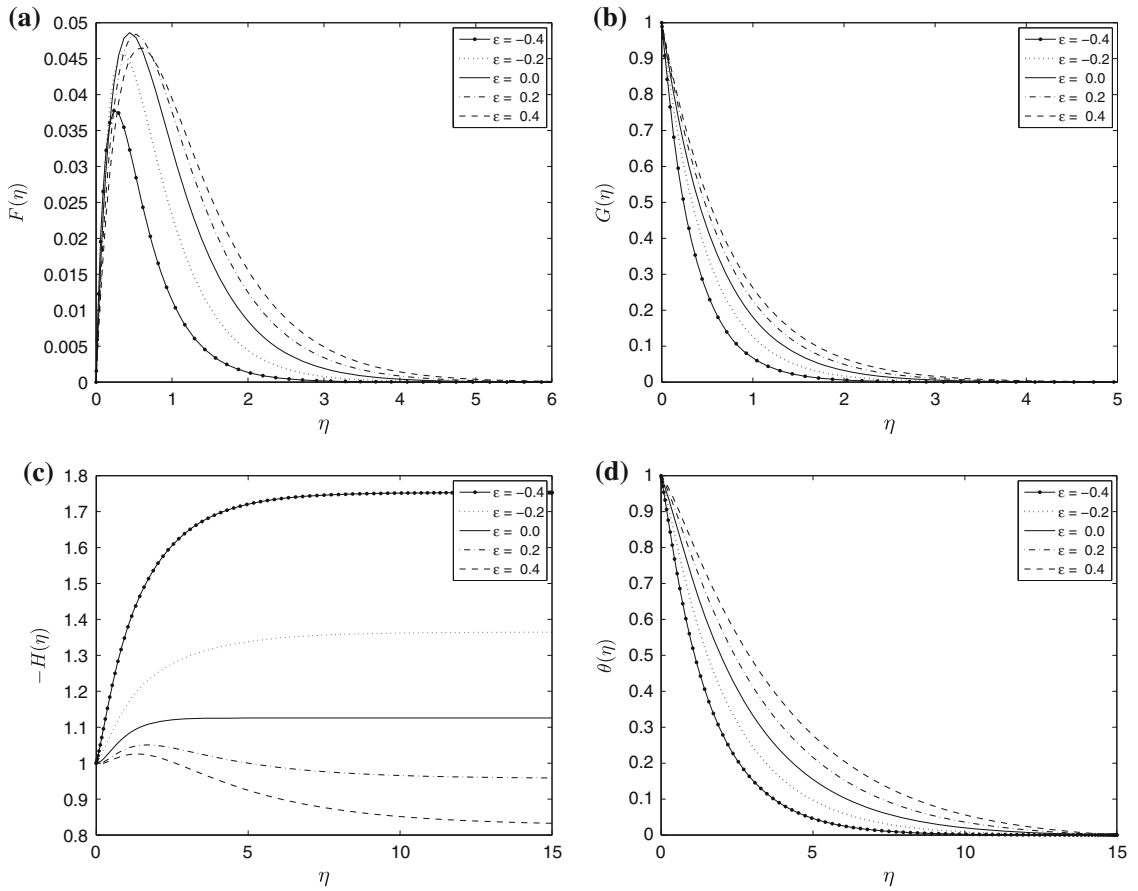

Fig. 2 Effect of variation in the relative temperature difference parameter ϵ on the (**a**) radial (**b**) tangential (**c**) axial and (**d**) temperature velocity profiles when $\beta_i = 0.5$, $\beta_e = 0.5$, $M = 0.5$, $Ec = 0.5$, $Da = 1.5$, $R_d = 1.5$ and $h_w = -1$

where $H_i(\eta)$, $F_i(\eta)$, F and $\theta_i(\eta)$ are unknown functions and $H_m(\eta)$, $F_m(\eta)$, $G_m(\eta)$ and $\theta_m(\eta)$ $(m \geq 1)$ are approximations which are obtained by recursively solving the linear part of the equation system that results from substituting (23) in the governing equations (12)–(16). The main assumption of the SLM is that H_i, F_i, G_i, and θ_i become increasingly smaller when i becomes large, that is

$$\lim_{i\to\infty} H_i = \lim_{i\to\infty} F_i = \lim_{i\to\infty} G_i = \lim_{i\to\infty} \theta_i = 0. \tag{24}$$

The initial guesses $H_0(\eta)$, $F_0(\eta)$, $G_0(\eta)$, and $\Theta_0(\eta)$ which are chosen to satisfy the boundary conditions (18) are taken to be

$$H_0(\eta) = h_w + e^{-\eta} - 1, \qquad F_0(\eta) = \eta)e^{-\eta}, \qquad G_0(\eta) = e^{-\eta}, \qquad \theta_0(\eta) = e^{-\eta}, \tag{25}$$

Thus, starting from the initial guesses, the subsequent solutions $H_i(\eta)$, $F_i(\eta)$, $G_i(\eta)$ and $\theta_i(\eta)(i \geq 1)$ are obtained by successively solving the linearized form of the equations which are obtained by substituting equation (**??**) in the governing equations (12–16) and neglecting the nonlinear terms containing $H_i(\eta)$, $F_i(\eta)$, $G_i(\eta)$ and $\theta_i(\eta)$ and its derivatives. The linearized equations to be solved are

$$a_{1,i-1}H_i'(\eta) + a_{2,i-1}H_i + a_{3,i-1}F_i + a_{4,i-1}\theta' i + a_{5,i-1}\theta_i = r_{1,i-1}, \tag{26}$$
$$b_{1,i-1}F_i'' + b_{2,i-1}F_i' + b_{3,i-1}F_i + b_{4,i-1}H_i + b_{5,i-1}G_i + b_{6,i-1}\theta_i' = r_{2,i-1}, \tag{27}$$
$$c_{1,i-1}G_i'' + c_{2,i-1}G_i' + c_{3,i-1}G_i + c_{4,i-1}H_i + c_{5,i-1}F_i' + c_{6,i-1}\theta_i' + c_{7,i-1}\theta_i = r_{3,i-1}, \tag{28}$$
$$d_{1,i-1}\theta_i'' + d_{2,i-1}\theta_i' + d_{3,i-1}\theta_i + d_{4,i-1}H + d_{5,i-1}F_i' + d_{6,i-1}F_i + d_{7,i-1}G_i' + d_{8,i-1}G_i = r_{4,i-1}, \tag{29}$$

subject to the boundary conditions

$$\left.\begin{aligned} H(0) = F(0) = G(0) = \theta(0) = 0 \\ H(\infty) = F(\infty) = G(\infty) = \theta(\infty) = 0 \end{aligned}\right\} \tag{30}$$

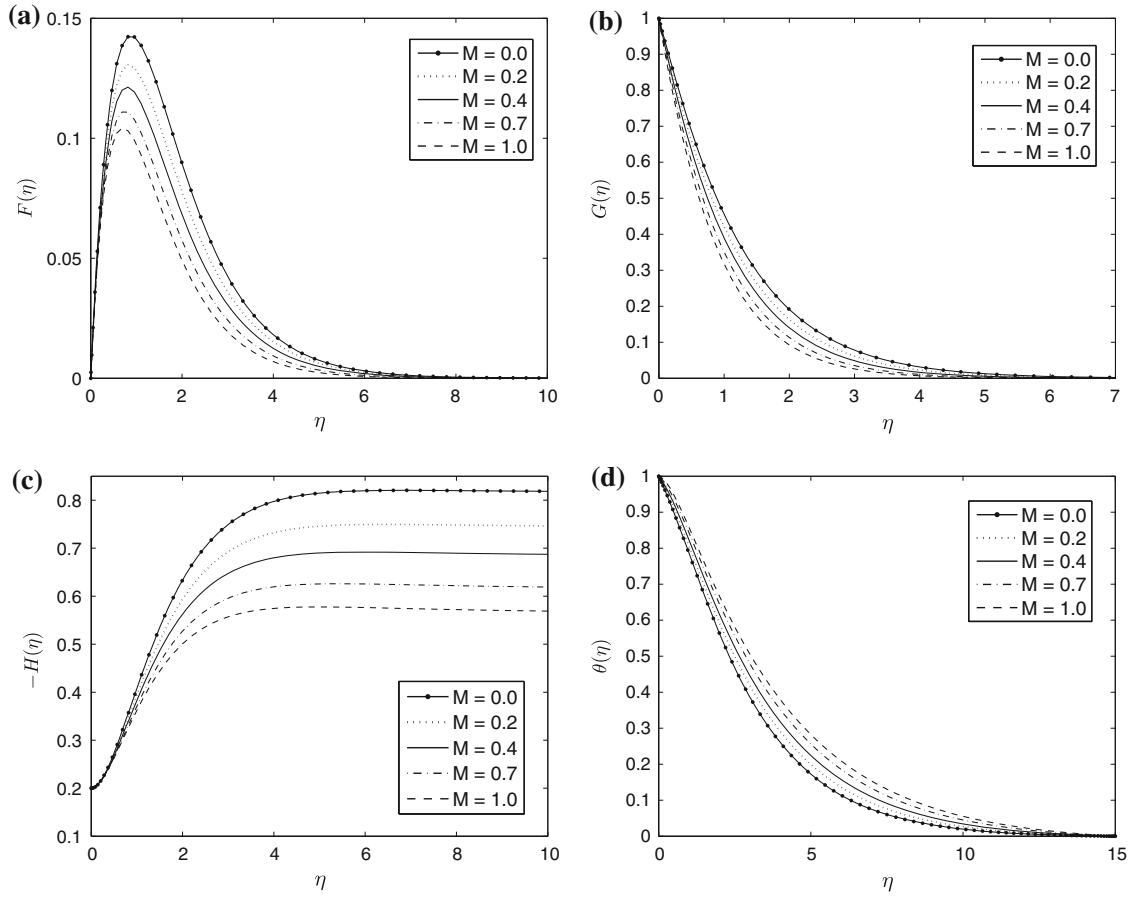

Fig. 3 Effect of variation in the magnetic field parameter M on the (**a**) radial (**b**) tangential (**c**) axial and (**d**) temperature velocity profiles when $\beta_i = 0.5$, $\beta_e = 0.5$, $\epsilon = 0.1$, $Ec = 0.5$, $Da = 10$, $R_d = 5$ and $h_w = -0.2$

where the coefficients' parameters $a_{k,i-1}$, $b_{k,i-1}$, $c_{k,i-1}$, $d_{k,i-1}$ and $r_{k,i-1}$ depend on H_{i-1}, F_{i-1}, G_{i-1}, θ_{i-1} and on their derivatives. Once each solution for H_i, F_i, G_i and θ_i has been found from interactively solving Eqs. (26)–(29) for each i, the approximate solutions for $H(\eta)$, $F(\eta)$, $G(\eta)$ and $\Theta(\eta)$ are obtained as

$$H(\eta) \approx \sum_{m=0}^{M} H_m(\eta), \quad F(\eta) \approx \sum_{m=0}^{M} F_m(\eta), \quad G(\eta) \approx \sum_{m=0}^{M} F_m(\eta), \quad \theta(\eta) \approx \sum_{m=0}^{M} \theta_m(\eta) \tag{31}$$

where M is the order of SLM approximations. Since the coefficient parameters and the right-hand side of Eqs. (26)–(29) for $i = 1, 2, 3\ldots$ are known(from previous iterations), the system (26)–(29) with the boundary conditions (30) can easily be solved using any analytical or numerical method. In this study we used the Chebyshev spectral collocation method [8,9,29]. This method is based on approximating the unknown functions by the Chebyshev interpolating polynomials in such a way that they are collocated at the Gauss–Lobatto points defined as

$$x_j = \cos\frac{\pi j}{N}, \qquad j = 0, 1, \ldots, N \tag{32}$$

In order to implement the method, the physical region $[0, \infty)$ is transformed into the region $[-1, 1]$ using the domain truncation technique in which the problem is solved on the interval $[0, L]$ instead of $[0, \infty)$. This leads to the mapping

$$x = \frac{2\eta}{L} - 1, \quad -1 \le x \le 1 \tag{33}$$

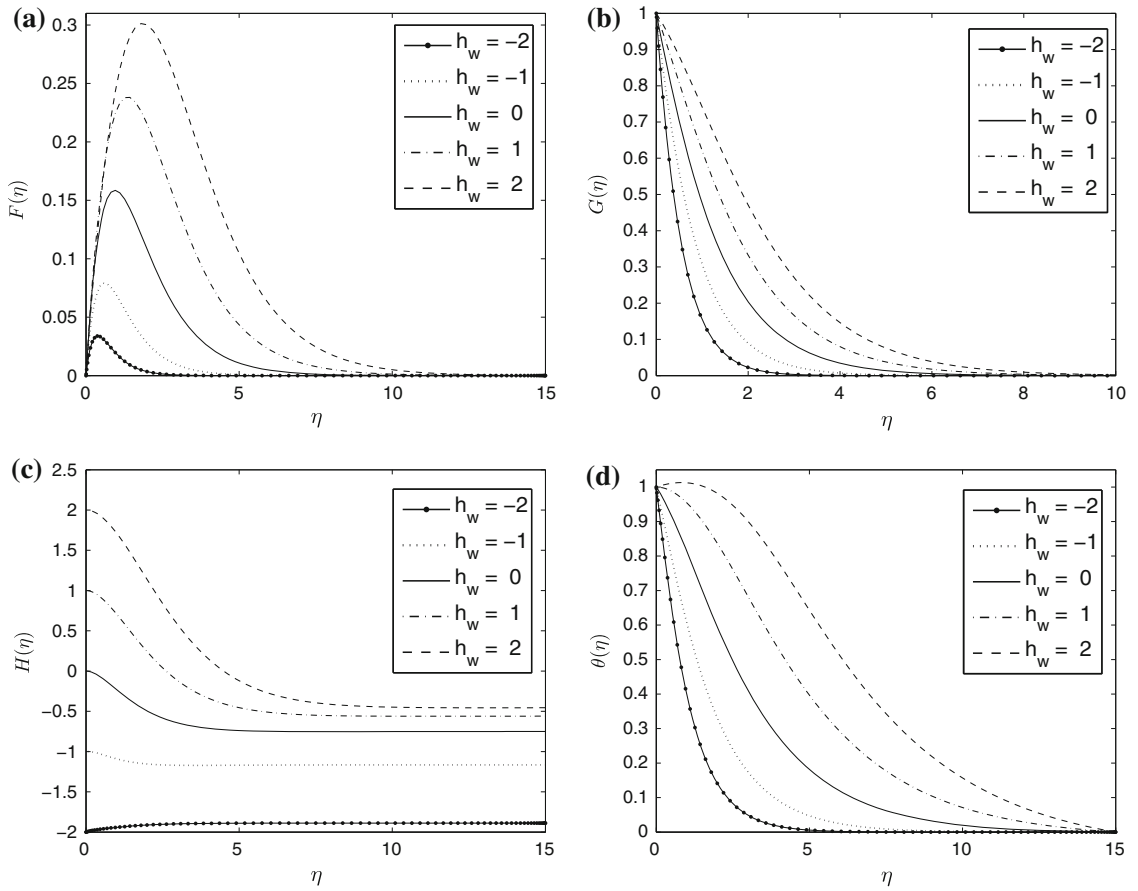

Fig. 4 Effect of variation in the suction and injection parameter h_w on the (**a**) radial (**b**) tangential (**c**) axial and (**d**) temperature velocity profiles when $\beta_i = 0.5$, $\beta_e = 0.5$, $\epsilon = 0.1$, $Ec = 0.5$, $Da = 15$, $R_d = 10$ and $M = 0.1$

where L is the scaling parameter used to invoke the boundary conditions at infinity. The unknown functions H_i, F_i, G_i and θ_i are approximated at the collocation points by

$$\left.\begin{aligned} H_i(x) &\approx \textstyle\sum_{k=0}^{N} H_i(x_k)T_k(x_j), \qquad F_i(x) \approx \textstyle\sum_{k=0}^{N} F_i(x_k)T_k(x_j) \qquad j = 0, 1, \ldots, N \\ G_i(x) &\approx \textstyle\sum_{k=0}^{N} G_i(x_k)T_k(x_j), \qquad \theta_i(x) \approx \textstyle\sum_{k=0}^{N} \theta_i(x_k)T_k(x_j) \qquad j = 0, 1, \ldots, N \end{aligned}\right\} \tag{34}$$

where T_k is the kth Chebyshev polynomial defined as

$$T_k(x) = \cos\left[k \cos^{-1}(x)\right] \tag{35}$$

The derivatives of the variables at the collocation points are represented as

$$\left.\begin{aligned} \tfrac{d^r H_i}{d\eta^r} &= \textstyle\sum_{k=0}^{N} \mathbf{D}^r_{kj} H_i(x_k), \qquad \tfrac{d^r F_i}{d\eta^r} = \textstyle\sum_{k=0}^{N} \mathbf{D}^r_{kj} F_i(x_k), \qquad j = 0, 1, \ldots, N \\ \tfrac{d^r G_i}{d\eta^r} &= \textstyle\sum_{k=0}^{N} \mathbf{D}^r_{kj} G_i(x_k), \qquad \tfrac{d^r \theta_i}{d\eta^r} = \textstyle\sum_{k=0}^{N} \mathbf{D}^r_{kj} \theta_i(x_k), \qquad j = 0, 1, \ldots, N \end{aligned}\right\} \tag{36}$$

where r is the order of differentiation and $\mathbf{D} = \frac{2}{L}\mathcal{D}$ with $\mathcal{D}$ being the Chebyshev spectral differentiation matrix whose entries are defined as (see for example, Canuto [8]);

$$\left.\begin{aligned} \mathcal{D}_{jk} &= \frac{c_j}{c_k}\frac{(-1)^{j+k}}{\xi_j - \xi_k} \qquad j \neq k;\ j, k = 0, 1, \ldots, N, \\ \mathcal{D}_{kk} &= -\frac{\xi_k}{2(1-\xi_k^2)} \qquad k = 1, 2, \ldots, N-1, \\ \mathcal{D}_{00} &= \frac{2N^2+1}{6} = -\mathcal{D}_{NN}. \end{aligned}\right\} \tag{37}$$

Substituting Eqs. (33)–(36) in (26)–(29) leads to the matrix equation

$$\mathbf{A}_{i-1}\mathbf{X}_i = \mathbf{R}_{i-1} \tag{38}$$

while the boundary conditions transform to

$$\left.\begin{aligned} H_i(x_0) = F_i(x_0) = G_i(x_0) = \theta_i(x_0) = 0 \\ H_i(x_N) = F_i(x_N) = G_i(x_N) = \theta_i(x_N) = 0 \end{aligned}\right\} \tag{39}$$

in which $\mathbf{A}_{i-1}$ is a $4(N+1) \times 4(N+1)$ square matrix while $\mathbf{X}_i$ and $\mathbf{R}_{i-1}$ are $4(N+1) \times 1$ column vectors defined by

$$\mathbf{A}_{i-1} = \begin{bmatrix} A_{11} & A_{12} & A_{13} & A_{14} \\ A_{21} & A_{22} & A_{23} & A_{24} \\ A_{31} & A_{32} & A_{33} & A_{34} \\ A_{41} & A_{42} & A_{43} & A_{44} \end{bmatrix}, \quad \mathbf{X}_i = \begin{bmatrix} \tilde{H}_i \\ \tilde{F}_i \\ \tilde{G}_i \\ \tilde{\theta}_i \end{bmatrix}, \quad \mathbf{R}_{i-1} = \begin{bmatrix} \mathbf{r}_{1,i-1} \\ \mathbf{r}_{2,i-1} \\ \mathbf{r}_{3,i-1} \\ \mathbf{r}_{4,i-1} \end{bmatrix} \tag{40}$$

with

$$\left.\begin{aligned} \tilde{H}_i &= \left[H_i(x_0), H_i(x_1), \ldots, H_i(x_{N-1}), H_i(x_N)\right]^T \\ \tilde{F}_i &= \left[F_i(x_0), F_i(x_1), \ldots, F_i(x_{N-1}), F_i(x_N)\right]^T \\ \tilde{G}_i &= \left[G_i(x_0), G_i(x_1), \ldots, G_i(x_{N-1}), G_i(x_N)\right]^T \\ \tilde{\theta}_i &= \left[\theta_i(x_0), \theta_i(x_1), \ldots, \theta_i(x_{N-1}), \theta_i(x_N)\right]^T \\ \mathbf{r}_{1,i-1} &= \left[r_{1,i-1}(x_0), r_{1,i-1}(x_1), \ldots, r_{1,i-1}(x_{N-1}), r_{1,i-1}(x_N)\right]^T \\ \mathbf{r}_{2,i-1} &= \left[r_{2,i-1}(x_0), r_{2,i-1}(x_1), \ldots, r_{2,i-1}(x_{N-1}), r_{2,i-1}(x_N)\right]^T \\ \mathbf{r}_{3,i-1} &= \left[r_{3,i-1}(x_0), r_{3,i-1}(x_1), \ldots, r_{3,i-1}(x_{N-1}), r_{3,i-1}(x_N)\right]^T \\ \mathbf{r}_{4,i-1} &= \left[r_{4,i-1}(x_0), r_{4,i-1}(x_1), \ldots, r_{4,i-1}(x_{N-1}), r_{4,i-1}(x_N)\right]^T \end{aligned}\right\} \tag{41}$$

and

$$\left.\begin{aligned} &A_{11} = a_{1,i-1}\mathcal{D} + [a_{2,i-1}], \quad A_{12} = [a_{3,i-1}], \quad A_{13} = [\mathbf{0}], \quad A_{14} = a_{4,i-1}\mathcal{D} + [a_{5,i-1}] \\ &A_{21} = [b_{4,i-1}], \quad A_{22} = b_{1,i-1}\mathcal{D}^2 + b_{2,i-1}\mathcal{D} + [b_{3,i-1}], \quad A_{23} = [b_{5,i-1}], \quad A_{24} = [b_{6,i-1}]\mathcal{D} \\ &A_{31} = [c_{4,i-1}], \quad A_{32} = [c_{5,i-1}], \quad A_{33} = c_{1,i-1}\mathcal{D}^2 + c_{2,i-1}\mathcal{D} + [c_{3,i-1}], \\ &A_{34} = c_{6,i-1}\mathcal{D} + [c_{7,i-1}], \quad A_{41} = [d_{4,i-1}], \quad A_{42} = d_{5,i-1}\mathcal{D} + [d_{6,i-1}], \\ &A_{43} = d_{7,i-1}\mathcal{D} + [d_{8,i-1}], \quad A_{44} = d_{1,i-1}\mathcal{D}^2 + d_{2,i-1}\mathcal{D} + [d_{3,i-1}] \end{aligned}\right\} \tag{42}$$

where $[\mathbf{0}]$ and $[\ ]$ are zero and diagonal matrices, respectively, of size $(N+1) \times (N+1)$ and $a_{k,i-1}, b_{k,i-1}, c_{k,i-1}, d_{k,i-1} (k = 1, 2, 3, 4)$ are diagonal matrix of size $(N+1) \times (N+1)$. After modifying the matrix system (38) to incorporate boundary conditions (39), the solution is obtained as

$$\mathbf{X}_i = \mathbf{A}_{i-1}^{-1}\mathbf{R}_{i-1} \tag{43}$$

5 Results and discussions

The results of solution of the system of transformed Eqs. (12)–(16) subject to the boundary conditions (18) were solved using SLM. In generating the results we used $L = 15$ and $Pr = 0.64$ which is the value of Prandtl number for a flue gas. To establish the validity of our numerical results adopted in the present investigation, we made a comparison of our calculated results with study of Kelson and Kelson and Desseaux [12] in Table 1 to the case of suction or injection velocity. The comparisons show excellent agreements, hence an encouragement for the use of the present numerical computations.

The effects of various values of the physical parameters on the radial, tangential, axial and temperature velocity profiles are plotted in Figs. 2, 3, 4, 5, 6, 7, 8 and 9. The obtained results of the present investigation have been implemented by comparisons with those of Frusteri and Osalusi [10], Osalusi and Sibanda [25], Osalusi et al. [24]. It found that our results are in very good agreement with theirs.

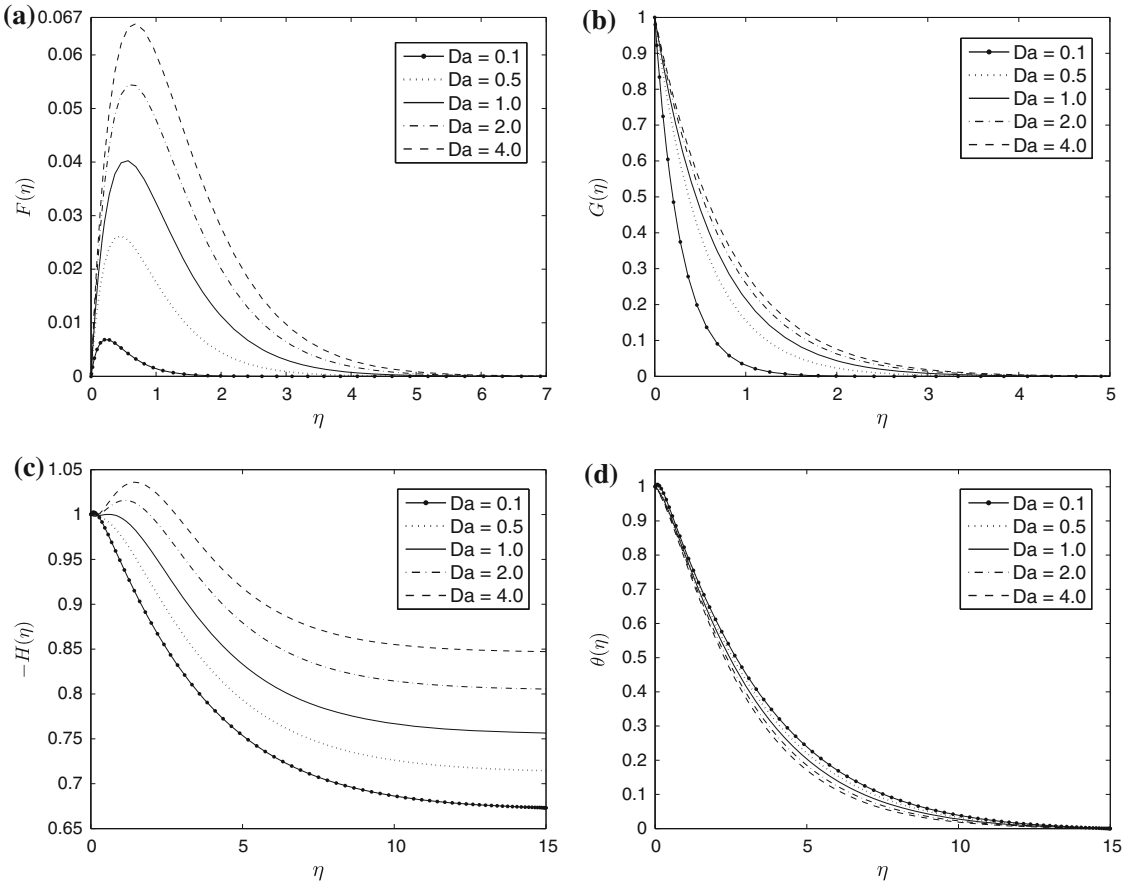

Fig. 5 Effect of variation in the Darcy number Da on the (**a**) radial (**b**) tangential (**c**) axial and (**d**) temperature velocity profiles when $\beta_i = 0.5$, $\beta_e = 0.5$, $\epsilon = 0.5$, $Ec = 0.5$, $M = 1$, $R_d = 5$ and $h_w = -1$

Figure 2a–d depict the effects of relative temperature differences ϵ on the radial, tangential and axial velocity and temperature profiles, respectively. The purpose of plotting these figures is to give a comparison between the constant property and variable property solutions. It is seen that in Fig. 2a, due to the existence of a centrifugal force the radial velocity attains a maximum value close to the disk for all values of ϵ. The maximum value of the velocity is attained in case of $\epsilon = 0$ (constant property). The radial velocity increases with the increase of the relative temperature difference parameter for most part of the boundary layer and at any fixed position. In Fig. 2b, it is seen that the tangential velocity increase with increasing values of ϵ while axial velocity (H) decreases with an increase in the relative temperature differences as observed in Fig. 2c. An increase in the value of ϵ enhances the non-dimensional temperature as we observed in Fig. 2d.

Figure 3a–d show the effect of the magnetic field parameter M on the velocity components (radial, tangential and axial) and temperature profiles. Imposition of a magnetic field generally to an electrically conducting fluid creates a drag like force called Lorentz force that has the tendency to slow down the flow around the disk at the same time increasing fluid temperature. As the magnetic field increases, the radial, tangential and axial velocity profiles decrease while the temperature profiles increase as shown in Fig. 3a–d, respectively.

Figure 4a–d showed the radial $F(\eta)$, axial $H(\eta)$, tangential $G(\eta)$ and the temperature $\theta(\eta)$ profiles for various values of suction and injection (h_w). It is seen that F, H, G and θ are increasing with increase in h_w, also we noted that for strong suction, the radial velocity is very small, the axial velocity is approximately constant while the tangential and temperature decay rapidly away from the surface.

The effects of Darcy number Da on the velocity components and temperature profiles are plotted in Fig. 5a–d. It is observed that for high Darcy number (corresponding to high permeability), the fluid velocity attains a maximum near the surface. An increasing Da increases the radial, tangential and axial velocities but decreases the temperature profile.

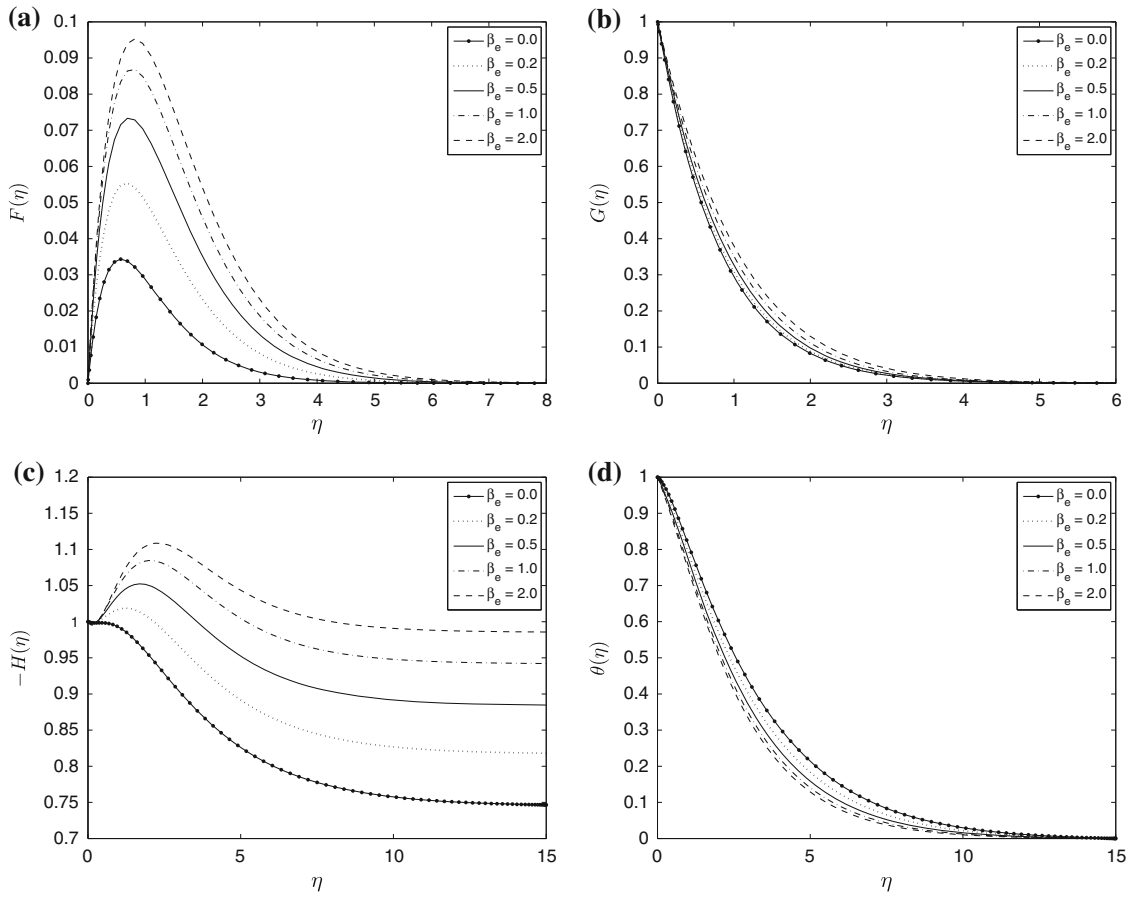

Fig. 6 Effect of variation in the Hall current parameter β_e on the (**a**) radial (**b**) tangential (**c**) axial and (**d**) temperature velocity profiles when $Da = 15$, $\beta_i = 1$, $\epsilon = 0.5$, $Ec = 0.5$, $M = 1$, $R_d = 5$ and $h_w = -1$

We illustrate the effect of various values of the Hall current parameter β_e on $F(\eta)$, $-H(\eta)$, $G(\eta)$ and $\theta(\eta)$ profiles in Fig. 6a–d. We observe that radial velocity F, tangential velocity G and axial velocity $-H$ increase while the temperature θ decreases as the Hall current parameter β_e increases.

Figure 7a–d describes the behavior of F, $-H$, G and θ against ion-slip parameter β_i. From these figures it is noted that increasing the ion-slip parameter β_e has an increasing effect on F, $-H$ and G while a decreasing effect on temperature. In general, the effect of Hall parameter on the flow and thermal fields is more notable than that of ion-slip parameter β_i. This is due to the fact that the diffusion velocity of the electrons is much larger than that of the ion.

The effect of different values of radiation parameter R_d on the axial velocity $-H$ and temperature profiles is displayed in Fig. 8a, b, respectively, it is observed from these figures that increase in the radiation parameter decreases the axial velocity and temperature distributions. Also it is observed that the temperature is maximum at the wall and asymptotically decreases to zero as $\eta \to \infty$.

Figure 9a–d describe the behavior of F, $-H$, G and θ profiles with changes in the values of the Eckert number Ec. From these figures we may conclude that in the presence of viscous dissipation and Ohmic heating, an increasing Ec increases the axial velocity $-H$, tangential velocity G, and temperature θ while decreasing the radial velocity F. The rise in the temperature, θ, is due to the heat created by viscous dissipation and compression work ($Ec \neq 0$). This behavior is shown in Fig. 9d.

Table 2 illustrates the effects of the parameters M, B_i, B_e, R_d, Ec and Da on the shear stress $F'(0)$, $H'(0)$, $-G'(0)$ and the rate of heat transfer $-\theta'(0)$. From Table 2 we observe that as the magnetic field parameter M increases, the shear stresses in the radial $F'(0)$ and tangential $-G'(0)$ directions increase, while the shear stress in axial $H'(0)$ direction and the rate of heat transfer $-\theta'(0)$ are decreased. This is due to the fact that an increase in the magnetic field decreases the radial and tangential velocities (see Fig. 3a, c), but increases the temperature distribution (see Fig. 3d. Also, it was observed that in Table 2, an increase in

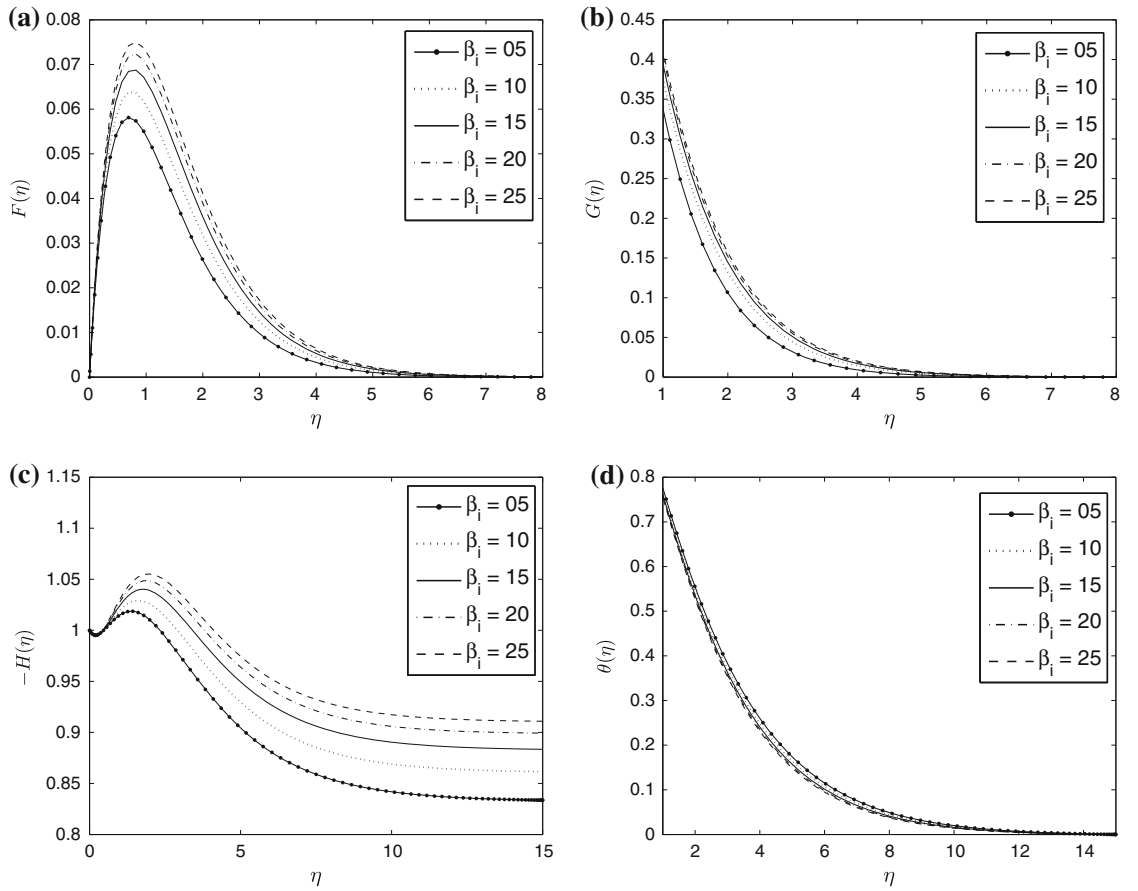

Fig. 7 Effect of variation in the ion-slip parameter β_i on the (**a**) radial (**b**) tangential (**c**) axial and (**d**) temperature velocity profiles when $Da = 10$, $\beta_e = 0.5$, $\epsilon = 0.5$, $Ec = 0.5$, $M = 2$, $R_d = 5$ and $h_w = -1$

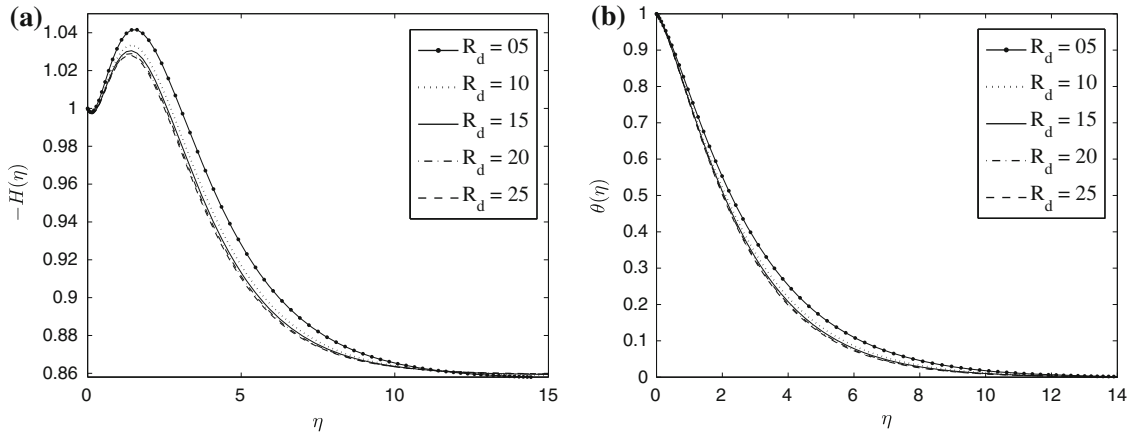

Fig. 8 Effect of variation in the radiation parameter R_d on the (**a**) axial velocity and (**b**) temperature profiles when $Da = 5$, $\beta_e = 0.5$, $\beta_i = 0.5$, $\epsilon = 0.5$, $Ec = 0.5$, $M = 1$ and $h_w = -1$

the values of ion-slip B_i decreases both the shear stresses in the radial $F'(0)$ and tangential $-G'(o)$ directions while the rate of heat transfer increases. Table 2 reveals that the radial $F'(0)$ and axial $H'(0)$ shear stresses as well as heat transfer coefficient $-\theta'(0)$ increase with increase in the values of Hall parameter B_e but decreases the tangential shear stress $-G'(0)$. Further, we observe that radial skin friction and rate of heat transfer decrease with Ec increases but the tangential skin friction increases. The heat transfer coefficient decreases due to heat

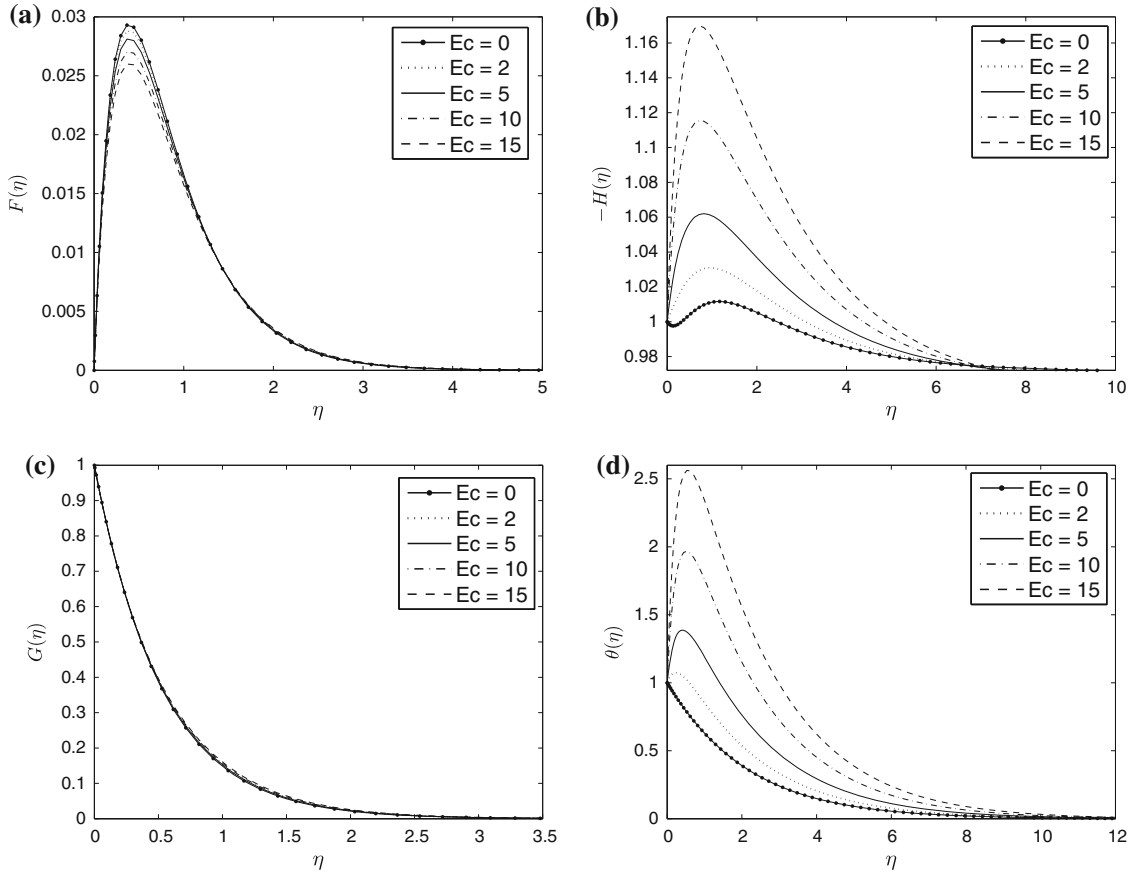

Fig. 9 Effect of variation in the Eckert number Ec on the (**a**) radial (**b**) tangential (**c**) axial and (**d**) temperature velocity profiles when $Da = 1$, $\beta_e = 0.1$, $\beta_i = 0.2$, $\epsilon = 0.1$, $M = 1$, $R_d = 5$ and $h_w = -1$

created by both viscous dissipation and compression work ($Ec \neq 0$). Also Table 2 indicates that increasing thermal radiation R_d has an increasing effect on $F'(0)$, $H'(0)$ and $-\theta'(0)$ while there is a decreasing effect on $-H'(0)$.

6 Conclusions

In this study, we have examined the effect of Ohmic heating and viscous dissipation on MHD porous rotating disk taking into account the variable properties of the fluid in the presence of Hall current and radiation. A similarity transformation reduced the governing partial differential equations into ordinary differential equations which were then solved using the SLM. The numerical results obtained are compared with previously published work available in the literature and the present results are found to be in excellent agreement. Numerical results illustrating interesting predicted phenomena were presented graphically and in tabular form. The main conclusions emerging from this study are as follows:

(i) The effect of the Lorentz force or the usual resistive effect of the magnetic field on the velocity components is apparent. The presence of magnetic field acts to reduce the velocity of fluid particles, whereas the temperature in fluid is enhanced. Also it has been observed that the radial and tangential skin-friction values decrease with increase in the magnetic parameter.

(ii) The radial, tangential and axial velocity profiles increase while the temperature decreases with the increasing values of Hall current and ion-slip parameters.

(iii) The viscous dissipation parameter or Eckert number Ec has marked effect on the flow. The axial, tangential and temperature velocity profiles increase while radial velocity profiles decrease with the increasing values of viscous dissipation.

Table 2 Numerical values of the radial, axial, tangential skin-friction coefficients and the rate of heat transfer coefficient for various values of M, B_i, B_e, R_d, Ec and Da with $h_w = -1$ and $\epsilon = 0.3$

M	B_i	B_e	R_d	Ec	Da	$F'(0)$	$H'(0)$	$-G'(0)$	$-\theta'(0)$
0.1	0.2	0.1	2.0	0.5	5.0	0.273948	0.045900	1.010687	0.198900
0.5	0.2	0.1	2.0	0.5	5.0	0.239841	0.033170	1.199004	0.143738
1.0	0.2	0.1	2.0	0.5	5.0	0.217671	0.021387	1.397108	0.092676
1.5	0.2	0.1	2.0	0.5	5.0	0.205712	0.012023	1.567291	0.052102
0.1	0.1	0.1	2.0	0.5	5.0	0.273882	0.045848	1.011209	0.198674
0.1	0.3	0.1	2.0	0.5	5.0	0.274015	0.045951	1.010175	0.199120
0.1	0.5	0.1	2.0	0.5	5.0	0.274146	0.046049	1.009179	0.199546
0.1	0.7	0.1	2.0	0.5	5.0	0.274277	0.046143	1.008221	0.199952
0.1	0.2	0.1	2.0	0.5	5.0	0.273948	0.045900	1.010687	0.198900
0.1	0.2	0.2	2.0	0.5	5.0	0.278824	0.046262	1.010552	0.200470
0.1	0.2	0.3	2.0	0.5	5.0	0.283160	0.046631	1.009587	0.202069
0.1	0.2	0.4	2.0	0.5	5.0	0.286876	0.046990	1.008010	0.203621
0.1	0.2	0.1	1.0	0.5	5.0	0.272956	0.035527	1.011757	0.153952
0.1	0.2	0.1	5.0	0.5	5.0	0.274917	0.056778	1.009652	0.246037
0.1	0.2	0.1	10.0	0.5	5.0	0.275342	0.061784	1.009201	0.267733
0.1	0.2	0.1	15.0	0.5	5.0	0.275499	0.063667	1.009035	0.275889
0.1	0.2	0.1	2.0	0.1	5.0	0.274590	0.066583	1.009941	0.288527
0.1	0.2	0.1	2.0	0.3	5.0	0.274269	0.056246	1.010313	0.243732
0.1	0.2	0.1	2.0	0.5	5.0	0.273948	0.045900	1.010687	0.198900
0.1	0.2	0.1	2.0	0.7	5.0	0.273628	0.035545	1.011062	0.154030
0.1	0.2	0.1	2.0	0.5	1.0	0.182634	0.031449	1.416147	0.136280
0.1	0.2	0.1	2.0	0.5	5.0	0.273948	0.045900	1.010687	0.198900
0.1	0.2	0.1	2.0	0.5	10.0	0.295094	0.048618	0.950520	0.210676
0.1	0.2	0.1	2.0	0.5	15.0	0.302957	0.049587	0.930038	0.214875

(iv) For the effect of the radiation parameter on the temperature distribution, it is seen that the temperature distribution decreases with the increasing values of radiation parameter and it increases the rate of heat transfer from the disk surface to the fluid.

(v) An increase in the Darcy number (increasing permeability) enhances radial, tangential and axial velocity profiles while the temperature reduces with increase in the Darcy number.

References

1. Ali, M.M.; Chen, T.S.; Armaly, B.F.: Natural convection-radiation interaction in boundary layer flow over horizontal surfaces. AIAA J. **22**, 1797–1803 (1984)
2. Arikoglu, A.; Ozkol, I.: On the MHD and slip flow over a rotating disk with heat transfer. Int. J. Numer Methods Heat Fluid Flow **28**(2),172–184 (2006)
3. Attia, H.A.: Unsteady MHD flow near a rotating porous disk with uniform suction or injection. Fluid Dyn. Res. **23**, 283–290 (1998)
4. Attia, H.A.: Unsteady flow and heat transfer of viscous incompressible fluid with temperature dependent viscosity due to a rotating disc in a porous medium. J. Phys. A Math. Gen. **39**, 979–991 (2006)
5. Awad, F.G.; Sibanda, P.; Motsa, S.S.; Makinde, O.D.: Convection from an inverted cone in a porous medium with cross-diffusion effects. Comput. Math. Appl. **61**, 1431–1441 (2011)
6. Benton, E.R.: On the flow due to a rotating disc. J. Fluid Mech. **24**(4), 781–800 (1965)
7. Cochran, W.G.: The flow due to a rotating disc. Proc. Camb. Phil. Soc. **30**, 365–375 (1934)
8. Canuto, C.; Hussaini, M.Y.; Quarteroni, A.; Zang, T.A.: Spectral Methods in Fluid Dynamics. Springer, Berlin (1988)
9. Don, W.S.; Solomonoff, A.: Accuracy and speed in computing the Chebyshev collocation derivative. SIAM J. Sci. Comput.**16**, 1253–1268 (1995)
10. Frusteri, F.; Osalusi, E.: On MHD and slip flow over a rotating porous disk with variable properties. Int. Commun. Heat Mass Transf. **34**, 492–501 (2007)
11. Jayaraj, S.: Thermophoresis in laminar flow over cold inclined plates with variable properties. Heat Mass Transf. **30**, 167–173 (1995)
12. Kelson, N.; Desseaux, A.: Note on porous rotating disk flow. ANZIAM J. **42**(E), C837–C855 (2000)
13. Makukula, Z.; Sibanda, P.; Motsa, S.S.: A note on the solution of the Von Karman equations using series and Chebyshev spectral methods. Boundary Value Probl., Article ID 471793, 17 pages (2010). doi:10.1155/2010/471793

14. Makukula, Z.; Motsa, S.S.: On new solutions for heat transfer in a visco-elastic fluid between parallel plates. Int. J. Math. Models Methods Appl. Sci. **4**(4), 221–230 (2010)
15. Makukula, Z.; Motsa, S.S.; Sibanda, P.: On a new solution for the viscoelastic squeezing flow between two parallel plates. J. Adv. Res. Appl. Math. **2**, 31–38 (2010)
16. Makukula, Z.; Sibanda, P.; Motsa, S.S.: A novel numerical technique for two-dimensional laminar flow between two moving porous walls. Math. Probl. Eng., 15 pages. Article ID 528956 (2010). doi:10.1155/2010/528956
17. Maleque, Kh.A.; Sattar, M.A.: The effects of variable properties and Hall current on steady MHD compressible laminar convective fluid flow due to a porous rotating disc. Int. J. Heat Mass Transf. **48**, 4963–4972 (2005)
18. Maleque, Kh.A.; Sattar, M.A.: Steady laminar convective flow with variable properties due to a porous rotating disk. J. Heat Transf. **127**, 1406–1409 (2005)
19. Millsaps, K.; Pohlhausen, K.: Heat transfer by laminar flow from a rotating disk. J. Aeronaut. Sci. **19**, 120–126 (1952)
20. Motsa, S.S.; Sibanda, P.: A new algorithm for solving singular IVPs of Lane-Emden type. In: Proceedings of the 4th International Conference on Applied Mathematics, Simulation and Modelling, NAUN International Conferences, Corfu Island, Greece, pp. 176–180 (2010)
21. Motsa, S.S.; Marewo, G.T.; Sibanda, P.; Shateyi, S.: An improved spectral homotopy analysis method for solving boundary layer problems. Boundary Value Probl. **3** (2011). doi:10.1186/1687-2770-2011-3
22. Motsa, S.S.; Sibanda, P.; Shateyi, S.: On a new quasi-linearization method for systems of nonlinear boundary value problems. Math. Methods Appl. Sci. **34**, 1406–1413 (2011)
23. Osalusi, E.; Sibanda, P.: On variable laminar convective flow properties due to a porous rotating disk in a magnetic field. Rom. J. Phys. **9**(10), 933–944 (2006)
24. Osalusi, E.; Side, J.; Harris, R.: The effects of Ohmic heating and viscous dissipation on unsteady MHD and slip flow over a porous rotating disk with variable properties in the presence of Hall and ion-slip currents. Int. Commun. Heat Mass Transf. **34**, 1017–1029 (2007)
25. Osalusi, E.; Sibanda, P.: On variable laminar convective flow properties due to a porous rotating disk in a magnetic field. Rom. J. Phys. **51**, 933–944 (2006)
26. Shateyi, S.; Motsa, S.S.: Variable viscosity on magnetohydrodynamic fluid flow and heat transfer over an unsteady stretching surface with hall effect. Boundary Value Probl. 20 pages. Article ID 257568 (2010). doi:10.1155/2010/257568
27. Sibanda, P.; Makinde, O.D.: On steady MHD flow and heat transfer past a rotating disk in a porous medium with ohmic heating and viscous dissipation. Int. J. Numer. Methods Heat Fluid Flow **20**(3), 269–285 (2010)
28. Sparrow, E.M.; Gregg, G.L.: Mass transfer, flow, and heat transfer about a rotating disk. ASME J. Heat Transf. **82**, 294–302 (1960)
29. Trefethen, L.N.: Spectral methods in MATLAB. SIAM (2000)
30. Turkyilmazoglu, M.: Purely analytic solutions of the compressible boundary layer flow due to a porous rotating disk with heat transfer. Phys. Fluids **21**, 106104 (2009)
31. Turkyilmazoglu, M.: The MHD boundary layer flow due to a rough rotating disk. ZAMM Z. Angew. Math. Mech. **90**(1), 72–82 (2010)
32. Von Karman, T.: Uber laminare und turbulente reibung. ZAMM **1**, 233–255 (1921)